

Zeptometer displacement sensing using a superconducting nonlinear interferometer

Dian Wahyu Utami*, Stojan Rebić, and Jason Twamley¹

¹Centre for Engineered Quantum Systems, Physics Department,
Macquarie University, North Ryde, NSW 2109, Australia

We propose a design for a superconducting nonlinear interferometer operating at microwave frequencies which allows the measurement of the optical nonlinearity η , with a precision which scales better than the Heisenberg-like limit as $\delta\eta \sim R^{-3/2}$, with R the quantification of resources. By designing the nonlinear optical element to possess physically moving parts we are able to use the superconducting nonlinear interferometer to measure the physical displacement r , of the moving parts to a spatial precision of $\delta(rt) \sim 10^{-21}$ m/Hz.

PACS numbers: 85.25.Hv, 78.47.nj, 78.47.N-, 06.30.Bp

Recent advances in technology have pushed further the limits of precision measurement. The standard limit of precision measurement is given by how the precision scales with the available resources R , such as measurement time or photon number (see [1] for a general discussion). By utilizing the quantum properties of a system one can reach a scaling of the precision δ that goes beyond the ‘‘Standard Quantum Limit’’ (SQL), eg. where $\delta \sim R^{-\alpha}$, $\alpha > \frac{1}{2}$, where R quantifies the resources required such as measurement time or photon number. The SQL or ‘‘shot-noise limit’’, is achieved when one attempts to measure an unknown phase using a linear interferometer with ‘‘classical’’ input states. This limit has now been pushed further to reach a Heisenberg-like limit of $\delta \sim 1/R$ by various methods. One way to achieve this is by utilizing entangled states [2, 3], as input states into a linear interferometer. Recent experiments approaching, and also reaching, this Heisenberg-like limit have been performed with linear interferometers using entangled input states [4, 5], and with feedback assisted methods using non-entangled input states [6, 7]. However, achieving a measurement precision scaling better than $1/R$ is possible when nonlinear and many-body interactions are included [8–10]. Such interactions are typically very difficult to find naturally and when found are usually very small when compared with other effects. Recently, a nonlinear interferometer using $\sim 2,000$ ^{87}Rb atoms in a Bose-Einstein condensate held in an optical lattice has experimentally achieved a precision better than the SQL [11]. In this work we propose a scheme for a superconducting nonlinear microwave interferometer which incorporates an ultra-large Kerr nonlinearity. We show, via homodyne measurements, how to utilize this nonlinear interferometer to achieve position displacement r , sensing with a precision which scales beyond the Heisenberg-like limit. We show that in-principle our scheme can achieve a measurement precision which scales as $\delta r \sim 1/\bar{n}^{3/2}$, where \bar{n} is the average photon number. Further, the degree of precision can be controlled by adjusting the microwave flux through the interferometer.

The ability to do precise metrology is gaining increasing importance. Quantum assisted metrology allows one to probe, for instance, motional displacements of nanoscopic cantilevers [12, 13], optical phase shifts [1], sensitive force sensing [14], or magnetic field sensing [15]. The gravitational

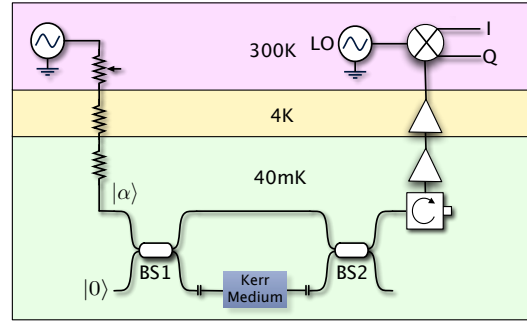


FIG. 1: Schematic circuit diagram of the nonlinear interferometer. One of the interferometer beams passes through a Giant-Kerr medium whose optical nonlinearity depends on a spatial separation within the superconducting circuit and this can be estimated via homodyne detection of an output beam.

wave community has a special interest in detecting motional displacement and currently holds the lead in sensitivity for displacement measurement. The state of the art gravitational wave detection by LIGO (Laser Interferometer Gravitational-Wave Observatory), which uses 4 km evacuated beamlines arranged in a high power optical interferometer, can attain a sensitivity of $\sim 10^{-22}$ m/ $\sqrt{\text{Hz}}$ [16]. Below we describe how it is possible to achieve this level of displacement measurement sensitivity in a laboratory setup using a superconducting circuit.

First, as shown in Fig. 1, a coherent microwave beam is attenuated, passed into a dilution fridge and is split into two beams by a low-temperature 90° microwave hybrid coupler (BS1), while the other input port is left empty (the vacuum). One output beam propagates through one arm of the interferometer while the other output passes through a Giant-Kerr nonlinear medium held within a bad-cavity (defined by the mirror capacitor: $\kappa \gg g, \gamma$, where κ is the decay rate of EM radiation from the cavity, g is the rate of coupling between the cavity and the ‘‘atom’’, and γ is the decay rate of the ‘‘atom’’). The two interferometer MW beams are recombined at a second low temperature hybrid coupler (BS2) and one output from this coupler is amplified by a microwave amplifier (e.g. HEMT), and analyzed by homodyne measurements at an IQ mixer combined with a Local Oscillator signal.

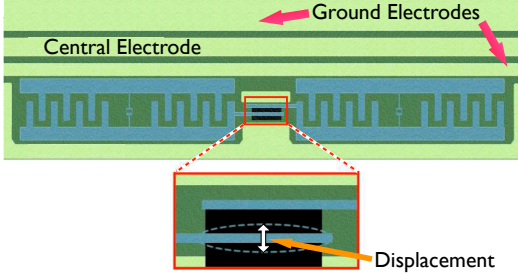


FIG. 2: Our proposed circuit, consisting two transmon qubits coupled together to a transmission line resonator. Coupling between the transmons is done via the parallel plate capacitors, where the relative distance separation between these two plates can change (as indicated in the inset).

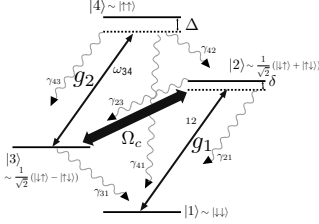


FIG. 3: 4 level scheme in N-Configuration created by coupling the two transmon to a transmission line resonator [19]

Our combined device acts like a nonlinear interferometer. Nonlinear interferometers were first introduced by Kitagawa and Yamamoto [17], and have been realized optically [18], and more recently via the nonlinear dynamics of Bose-Einstein condensates [11].

Our nonlinear Kerr effect is generated through a system that consists of two superconducting qubits coupled directly to each other and coupled to a transmission line resonator field mode creating a 4-level scheme in an N-configuration [19] (see Fig 3). Although any type of qubit is possible to be employed for this setup, we concentrate on capacitively coupled qubit for ease of adaptation to our application which details would be clear later on. Here we use transmon qubits instead of Cooper-Pair Boxes (CPB) to minimize dephasing noise. The quantised mode of the transmission line cavity couples to the N-system's transitions $|1\rangle \leftrightarrow |2\rangle$, and $|3\rangle \leftrightarrow |4\rangle$. In addition, the system is pumped by a classical field driving the transition $|3\rangle \leftrightarrow |2\rangle$ with a Rabi frequency Ω_c . The pump together with the quantum coupling to the transmission line generates electromagnetically induced transparency for the microwave tone on the $|2\rangle \leftrightarrow |1\rangle$ transition and consequently eliminates any spontaneous emission from level $|2\rangle$. The detuning Δ on the transition $|3\rangle \leftrightarrow |4\rangle$ is made larger than the linewidth of the excited state, thus effecting an ac-Stark shift on the ground state $|3\rangle$ which, in-turn, causes a giant nonlinear optical response for transmission line cavity mode.

It was shown earlier [19], that the nonlinearity depends on the coupling capacitance through the values of the detunings.

In this work we propose to provide this direct capacitive coupling via extended electrodes from each transmon. The simplest possible configuration is in the form of two capacitor plates as shown in the inset of Fig. 2. The detunings δ and Δ , in the N-system vary with the spatial separation between these two capacitor plates which in-turn change the Giant-Kerr optical nonlinearity experienced by the microwave tone held in the transmission line cavity. We consider a setup where the capacitor plate separation can change and take the initial setup to be where one plate is fixed in position while the other is movable (see inset of Fig. 2).

As shown in [20], the N-system, when interacting with the electromagnetic mode trapped in a cavity with loss rate κ , yields an effective nonlinear Kerr dynamics $H_{eff} \sim \hbar \eta a^\dagger{}^2 a^2$, with η the Giant-Kerr coefficient. In the limit when $g_{1,2} \ll \Omega_c$, one can find[21]:

$$\eta = \left(\frac{g_1}{\Omega_c} \right)^2 \left(\frac{g_2^2 \Delta}{\gamma_{43}^2 + \Delta^2} - \frac{g_1^2 \delta}{(\gamma_{21} + \gamma_{23})^2 + (\delta^2)} \right), \quad (1)$$

where we observe that the magnitude of the nonlinearity is independent of κ . The ratio η/κ determines if the system is in the photon blockade regime ($\eta/\kappa \gg 1$) or not, but it is important to stress that for large κ one can still have large η without a photon blockade. We model the microwave tone traveling wave interacting with the N-system as a driven very bad-cavity containing the N-system and consider the limit $\kappa \rightarrow \infty$. In our simulations we consider a driving tone mode with $E_p = 2\pi \times 5$ MHz, $\Delta = \delta = -2\pi \times 60$ MHz, $g_1 = g_2 = 2\pi \times 100$ MHz, $\Omega_c = 2\pi \times 1500$ MHz and the classical driving field Ω_c is resonant on the $|2\rangle - |3\rangle$ transition.

We model the input tone to the interferometer as a coherent state $|\alpha\rangle$ which is split by 90° hybrid coupler (beam splitter) whose action on the incoming field is $\hat{U}_{BS} = e^{-i\theta(\hat{a}^\dagger \hat{b} + \hat{a} \hat{b}^\dagger)t}$, where as usual, \hat{a} and \hat{b} describes the two incoming fields to the beamsplitter and θ describes the phase between the transmitted and reflected field. We now consider one arm of the interferometer to experience a linear phase shift ϕ in addition to the Giant Self-Kerr interaction and this corresponds to the operator $\hat{U}_\eta = e^{-i(\phi \hat{a}^\dagger \hat{a} + \eta (\hat{a}^\dagger)^2 \hat{a}^2)t}$. We recombine the two beams using another hybrid coupler. Taking the input quantum state to the nonlinear interferometer to be $|\psi_{in}\rangle = |\alpha, 0\rangle$, we obtain the output state as $|\psi_{out}\rangle = \hat{U}_{BS} \hat{U}_\eta \hat{U}_{BS} |\alpha, 0\rangle$.

Via a homodyne detection of one of the output modes we effectively measure the quadratures: $\hat{X}_1 = (\hat{a} + \hat{a}^\dagger)/2$, $\hat{Y}_1 = -i(\hat{a} - \hat{a}^\dagger)/2$.

From just one of these of the output quadratures, we can estimate the unknown nonlinear phase with a precision of:

$$\delta(\eta t) = \frac{\Delta X}{|d\langle \hat{X} \rangle / d(\eta t)|} \quad (2)$$

where $\Delta X = \sqrt{\langle \hat{X}^2 \rangle - \langle \hat{X} \rangle^2}$ is the variance in the measured quantity \hat{X} quadrature or similarly for the \hat{Y} quadrature. Note that our interferometer scheme uses homodyne detection which is regularly used in superconducting circuits rather than

photon counting, which has only recently been developed in superconducting systems [22].

The quantum limit of measurement using interferometry was first explored by Caves [23]. We can derive an analytical expression for the precision of estimating ηt , using either the \hat{X} or \hat{Y} quadratures:

$$\delta(\eta t)(\hat{X}) = \frac{e^{2\bar{n}\sin(\eta t)^2} \sqrt{1 + \bar{n} - 2A \cos^2(\phi_1) + B}}{2\sqrt{2\bar{n}^{3/2}} |\sin(\phi_1 + 2\eta t)|} \quad (3)$$

$$\delta(\eta t)(\hat{Y}) = \frac{e^{2\bar{n}\sin(\eta t)^2} \sqrt{1 + \bar{n} - 2A \sin^2(\phi_1) - B}}{2\sqrt{2\bar{n}^{3/2}} |\cos(\phi_1 + 2\eta t)|} \quad (4)$$

with $A = e^{-4\bar{n}\sin(\eta t)^2} \bar{n}$, and $B = e^{\bar{n}(-1+\cos(4\eta t))} \bar{n} \cos(\phi_2)$, where $\phi_1 = \phi t + \bar{n} \sin(2\eta t)$, $\phi_2 = 2(\delta + \eta)t + \bar{n} \sin(4\eta t)$, and \bar{n} is the average photon number associated with the initial coherent state $|\alpha\rangle$.

In the limit of small time $\bar{n}\eta t \ll 1$, this leads to a precision δ which scales as $2\bar{n}^{-3/2}$. This precision scales better than the Heisenberg-like scaling of $1/\bar{n}$. We now utilize this fact to perform displacement measurement by arranging the nonlinearity to be highly sensitive to a spatial displacement.

We begin by studying the dependence of the nonlinearity on the capacitive coupling and particularly on the separation between the two plates. As an example, we take the two plates as parallelepipeds of a dimensions $(w, l, t) = (200, 70, 0.16)\mu\text{m}$. The coupling capacitance between the two transmons, each with self capacitance of 100 fF, now depends on the separation r , between these two capacitor plates. We consider the Josephson energy of each junction to be $E_j = 2\pi \times 15$ GHz [24]. We consider the transmons to couple to the transmission line cavity with couplings $g_1 = g_2 = 2\pi \times 100$ MHz. From this we can numerically calculate the Giant-Kerr nonlinearity for various separation distances, as shown in Fig. 5a.

As can be seen from Fig. 4a, a nonlinearity of η/κ in the order of $10^3 - 10^4$ can be obtained. Note that the graph is of ratio of η to κ , thus dependence of the nonlinearity on the distance can be achieved independently of κ .

The precision one achieves when measuring the nonlinear phase via the quadrature measurement (equation (4)), can be translated into a precision to estimate small changes in the plate separation r , as

$$\delta(rt) = \frac{\Delta X}{d\langle\hat{X}\rangle/d(rt)} = \frac{\Delta X}{\frac{d\langle\hat{X}\rangle}{d(\eta t)} \frac{d(\eta t)}{d(rt)}} = \frac{\delta(\eta t)}{d\eta/dr} \quad (5)$$

The r dependence of $\delta(rt)$ can be plotted (Fig. 4b), and we note that the precision increases as the separation between the two plates is reduced and has a sharp minimum when the separation is comparable to the thickness of the capacitor plates. In the following we will investigate the precision of estimating position displacements when the two plates are separated by a fraction of a micron, a separation distance that is experimentally feasible.

From equations (4) and (5), we find that measurement sensitivity increases with increasing photon number (Fig. 4b).

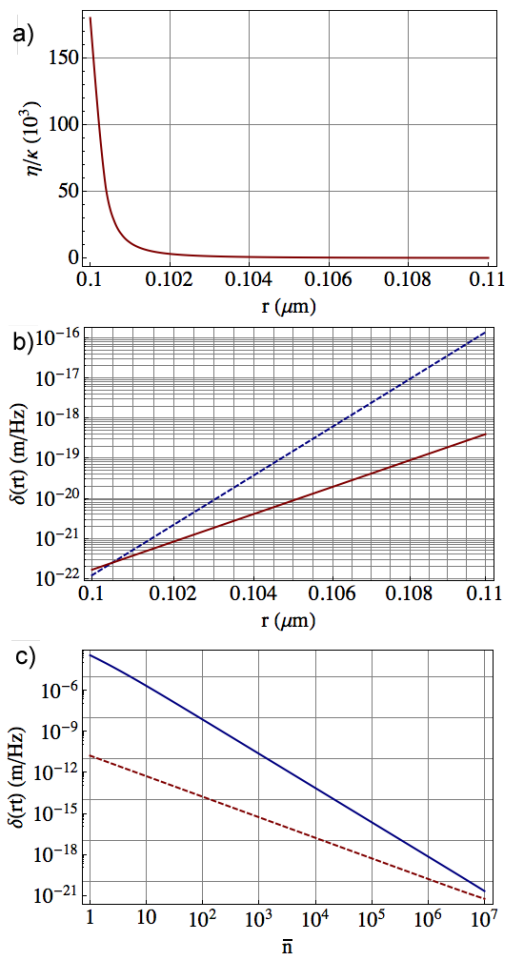


FIG. 4: (Color online) Dependence of the precision on various variable in the setup. a). Graph of the Giant-Kerr nonlinearity vs. r when the default plate separation is set at $d = r_0 + r$ where $r_0 = 1.01\mu\text{m}$. b). Graph of the precision displacement measurement using the X (solid blue) and Y (dashed red) quadratures as a function of r . c). Graph of the precision displacement measurement vs. the average photon number of the input state for X (solid blue) and Y (dashed red) quadrature estimation

From Fig. 4c, we can see that we can reach a precision on the order of $\delta(rt) \approx 10^{-21}\text{m/Hz}$ for $\bar{n} \approx 10^7$, this is a precision scaling comparable to LIGO. We do not consider when $\bar{n} > 10^7$ as the superconducting waveguides themselves display nonlinear effects. The sensitivity for lower photon number input states are also quite remarkable. Note that we have employed a highly lossy cavity to mimic the traveling wave interacting with the N-system and we find that the sensitivity can be optimized by changing the transmon capacitances given a range of displacements. Although we have not yet treated noise in this system, we believe that this will not hinder the workability of our scheme.

Current state of the art on-chip displacement transducers are able to measure $\delta r \sim 1\text{pm}/\sqrt{\text{Hz}}$ at room temperature [25] while commercial cantilevers are able to measure $50 - 200\text{fN}/\sqrt{\text{Hz}}$ [26]. More recently displacement sensitivity of

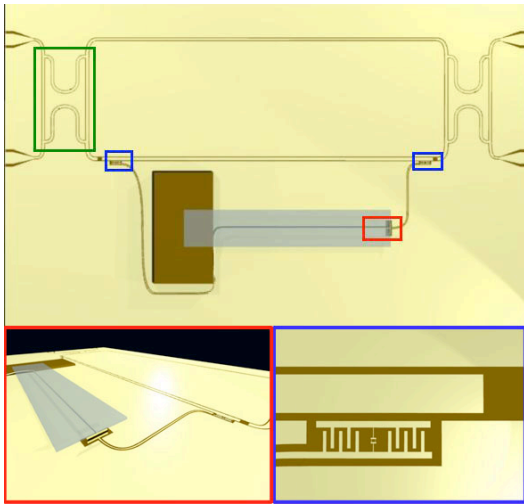


FIG. 5: Setup as gravimeter, showing the signal split into two parts by the 90 degrees hybrid coupler (green), the two transmon coupled to the transmission line (blue) and the two capacitive plates, one on a moving cantilever (red). Lower left figure showing the two capacitive plates, one on the cantilever, right lower figure showing the transmon in close-up

$250 \times 10^{-18} \text{ m}/\sqrt{\text{Hz}}$ was obtained using SiN nanomechanical oscillator [27].

By attaching our displacement sensor to a cantilever we can also transform our setup into a mass sensing detector. We consider a setup where the coupling capacitance is given by two plates being brought together by the motion of a cantilever. If this cantilever is massive it will move as a result of a gravitational force due to another object. One plate is arranged on the cantilever end and wired to one transmon, whilst the other plate is fixed on the substrate and connected to the other transmon (see lower left of Fig. 5). Considering a rectangular cantilever of $(l, w, t) = (200, 70, 0.8) \mu\text{m}$ made of Silicon Nitride ($\rho = 3184 \text{ kg/m}^3$, $E = 250 \text{ GPa}$), one has a spring constant of $k = 0.3 \text{ N/m}$. This type of cantilever is commercially available and often used in Atomic Force Microscopy (AFM) [26, 28]

An additional mass (for instance an additional cube of gold of $50 \mu\text{m}$ side-length) may be attached to the top of the cantilever to increase the deflection of the cantilever to gravitational forces. With displacement measurement precision of 10^{-22} m/Hz , our system would be able to detect a change in force of $6.6 \times 10^{-17} \text{ N/Hz}$, equivalent to a force produced by a 1 kg mass at a distance of 1m away from our cantilever over one second. This is also equivalent to the ability of equivalently detecting $10^{-9} g$ changes in gravity. The current most precise gravimeter available is a superconducting gravimeter which is able to detect changes in gravity with a sensitivity of $10^{-12} g$ [29].

We assess the effect of zero point motion on our movable cantilever. The zero point displacement is given by $x_{zpm} = \sqrt{\hbar/2m\Omega}$, where Ω the frequency of the cantilever, which, for our setup gives a value of $x_{zpm} \approx 10^{-15} \text{ m}$ with

the additional mass attached to our cantilever. In using our system directly to sense the displacement of LIGO mirror of 10.7 kgs oscillating at a frequency of 1 Hz, the x_{zpm} will reduce to $\approx 10^{-18} \text{ m}$. This can be further reduced by one or two order of magnitude when parametric squeezing is applied in one of the quadrature [30]. Thus our sensor can be used to yield near-zeptometer/Hz displacement sensing for the LIGO mirrors.

In summary, the scheme presented here allows super-Heisenberg-like scaling in the sensitivity of spatial separation measurement. We specifically show the implementation of our scheme in a superconducting circuit for displacement measurement with possible applications to gravimetry. Our technique, using a nonlinear interferometer, perhaps also can be used to ultra-sensitively measure the changes in the probe height in low temperature scanning probe microscopy.

We acknowledge support from the ARC Centre for Quantum Computer Technology, the European Union FET Projects QUANTIP & Q-ESSENCE and the ARC Discovery Project DP0986932.

-
- [1] Higgins, B. L., Berry, D. W., Bartlett, S. D., Wiseman, H. M. & Pryde, G. J. *Nature* **450**, 393 (2007).
 - [2] Giovannetti, V., Lloyd, S. & Maccone, L. *Science* **306**, 1330–1336 (2004).
 - [3] Berry, D. W. & Wiseman, H. M. *Phys. Rev. Lett.* **85**, 5098 (2000).
 - [4] Mitchell, M. W., Lundeen, J. & Steinberg, A. *Nature* **429**, 161–164 (2004).
 - [5] Leibfried, D. *et al. Science* **304**, 1476 (2004).
 - [6] Berry, D. W. & Wiseman, H. M. *Nat. Phot.* **3**, 317 (2009).
 - [7] Schliesser, A., Arcizet, O., Rivière, R., Anetsberger, G. & Kippenberg, T. J. *Nat. Phys.* **5**, 509 (2009).
 - [8] Boixo, S. *et al. Phys. Rev. Lett.* **101**, 040403 (2008).
 - [9] Woolley, M. J., Milburn, G. J. & Caves, C. M. *New J. Phys.* **10**, 5018 (2008).
 - [10] Choi, S. & Sundaram, B. *Phys. Rev. A* **77**, 53613 (2008).
 - [11] Gross, C., Zibold, T., Nicklas, E., Estève, J. & Oberthaler, M. K. *Nature* **464**, 1165 (2010).
 - [12] Teufel, J. D., Donner, T., Castellanos-Beltran, M. A., Harlow, J. W. & Lehnert, K. W. *Nat. Nano.* **4**, 820 (2009).
 - [13] Rocheleau, T. *et al. Nature* **463**, 72 (2010).
 - [14] Regal, C. A., Teufel, J. D. & Lehnert, K. W. *Nat. Phys.* **4**, 555–560 (2008).
 - [15] Jones, J. A. *et al. Science* **324**, 1166 (2009).
 - [16] Abadie, J. *et al. Phys. Rev. D* **81**, 102001 (2010).
 - [17] Kitagawa, M. & Yamamoto, Y. *Phys. Rev. A* **34**, 3974 (1986).
 - [18] Matsuda, N., Shimizu, R., Mitsumori, Y., Kosaka, H. & Edamatsu, K. *Nat. Phot.* **3**, 95 (2009).
 - [19] Rebic, S., Twamley, J. & Milburn, G. J. *Phys. Rev. Lett.* **103**, 150503 (2009).
 - [20] Schmidt, H. Imamoğlu, A. *Opt. Lett.* **23**, 1007–1009 (1998).
 - [21] Rebic, S., Tan, S., Parkins, A. & Walls, D. *J. Opt. B: Quantum Semiclass. Opt.* **1**, 490 (1999).
 - [22] Johnson, B. R. *et al. Nat. Phys.* **6**, 663 (2010).
 - [23] Caves, C. M. *Phys. Rev. D* **23**, 1693 (1981).
 - [24] Majer, J. *et al. Nature* **449**, 443 (2007).
 - [25] Unterreithmeier, Q. P., Faust, T., Manus, S. & Kotthaus, J. P.

Nano Lett. **10**, 887 (2010).

- [26] Olympus specification of available micro cantilevers.
<http://probe.olympus-global.com/en/en/specnitrideE.html>
- [27] Anetsberger, G. *et al.* *arXiv:quant-ph/1003.3752v1* (2010).
- [28] Nanoscience website of various available micro cantilever.
<http://store.nanoscience.com>
- [29] Shiomi, S. *Prog. Theor. Phys. Suppl.* **172**, 61 (2008).
- [30] Blencowe, M. P & Wybourne, M. N., *Physica B* **280**, 555 (2000).